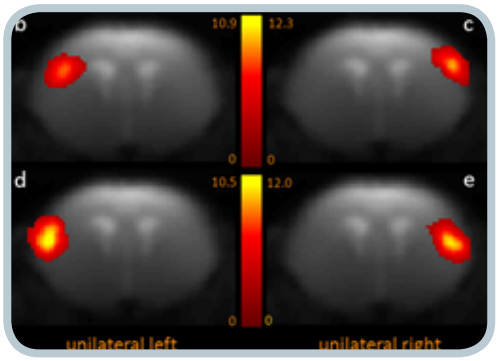

Fine-grained mapping of mouse brain functional connectivity with resting-state fMRI

Anna Mechling, Jürgen Hennig, Dominik von Elverfeldt and Laura Adela Harsan

Department of Radiology, Medical Physics, University Hospital Freiburg, Germany

Resting state functional MRI (rs-fMRI) opened a new era in the neuroimaging field (Biswal et al., 1995) marking a paradigm shift towards the concept of integrated whole brain functional networks, as opposed to locating isolated functional brain areas activated by a certain stimulus paradigm. Detecting spontaneous, low frequency (<0.1Hz) fluctuations in Blood Oxygen Level Dependent (BOLD) signal, and their temporal correlations (Biswal, 2012), the technique provides a unique non-invasive window into the intrinsic whole brain functional connectivity architecture. Over time, the technique's ability to decipher brain pathology patterns was proven (Castellazzi et al., 2014; Zhou et al., 2014; Nathan et al., 2015; Odish et al., 2015) and is now extensively used in human brain investigations (Sporns et al., 2005; Van Essen et al., 2013). The characterization of consistent and robust resting state networks in rodents progressively evolved as well, but despite encouraging initial results (Jonckers et al., 2011) fine-grained mapping of the mouse brain resting state networks in mice remains an underexplored area. This is in contrast to the widespread use of this species in experimental neuroscience for modeling human neurological disorders. Therefore, uncovering information related to the remodeling of brain networks in these models could contribute to a change in the view on brain disorder pathophysiology and finally establishing imaging biomarkers.

The challenges of rs-fMRI in small animals are numerous and relate to the necessity of fast acquisition methods at high-resolution while ensuring stable physiological parameters throughout the experiment. Here we show that taking advantage of the latest state-of-the-art technology for mouse MRI – the CryoProbe, a fine-grained non-invasive insight into the mouse brain functional "connectome" is possible. Due to the cooling of the probe and its electronics, a signal to noise increase of a factor of >2 is achieved.

Based on this data, we identify reliable patterns of the mouse brain intrinsic brain functional network architecture. Our approach relies on the blind source spatial separation of the BOLD signal via group level independent component analysis (ICA) combined with graph theoretical analysis. We demonstrate that under medetomidine light sedation (adapted from Pawela et al., 2009) the basic modular properties known from the human brain were reproduced in the mouse and the network has the hallmarks of a small-world efficient network. We additionally distinguish the highly connected mouse brain areas, highlighting their importance as relays of the functional connectivity. This type of information is essential in translational studies, bridging the gap between preclinical and clinical investigations of functional connectome remodeling.

Experimental Protocol

For further details on the experimental protocol see (Mechling et al., 2014, and http://www.uniklinik-freiburg.de/mr-en/research-groups/amir).

Animal stabilization and sedation: Rs-fMRI was performed in 8 to 9 weeks old C57BL/6N female mice (n = 13). Moderate sedation was induced by application of the α2-adreno-receptor agonist medetomidine (MD – Domitor, Pfizer, Karlsruhe, Germany) by a subcutaneous (sc) bolus injection (0.3 mg medetomidine per kg body weight). Fifteen minutes later, the animals received a continuous sc infusion of MD through a catheter placed at the mouse shoulder (0.6 mg per kg body weight). Throughout the imaging session, body temperature, respiration rate, blood oxygen saturation and heart rate were monitored continuously and scans were only taken at stable parameters within physiological range.

Magnets and coils: Imaging is performed with a Bruker Biospec 7T small bore animal system, equipped with B-GA12S HP gradients. A ^{1}H mouse quadrature transmit/receive MRI CryoProbe and ParaVision 5.1 software (Bruker BioSpin MRI) were also used for data acquisition.

Shimming procedure: The magnetic field homogeneity is optimized by performing a localized shimming procedure on a volume of interest (7.5 x 10.5 x 15) mm^3 placed inside the mouse brain, using PRESS waterline spectroscopy protocol and FastMap procedures provided with Bruker ParaVision 5.1.

Sequence parameters: Single shot GE-EPI sequence was used for rs-fMRI acquisition {TE/TR = 10 ms/1700 ms}. The whole mouse brain [excluding the cerebellum] was covered using 12 slices of 0.7 mm slice thickness. With a field of view (FOV) of 1.92 x 1.2 cm^2 and an acquisition matrix of 128 x 80, the planar spatial resolution results in 150 x 150 μm^2. 200 volumes were recorded with slice acquisition in interlaced fashion for each run. Rs-fMRI scans were performed at 30 min after bolus injection.

Analysis: Preprocessing of the rs-fMRI data was done in Matlab and via Statistical Parametric Mapping (SPM8) fMRI tool. The pipeline included realignment of the 200 volumes to the first one for motion correction within one scan, spatial normalization to a chosen template to allow for group analysis and smoothing with a Gaussian kernel of FWHM 0.4 x 0.4 x 1 mm^3. An additional brain mask was created from the template and applied to all datasets before further processing.

Independent Component Analysis

Spatial Group Independent Component Analysis (ICA, Calhoun et al. 2001) with the GIFT toolbox (Group ICA of fMRI Toolbox – v1.3i, http://www.nitrc.org/projects/gift/) was carried out using Infomax algorithm. In this purely data-driven approach, the BOLD signal is divided into components resulting from sources which are regarded as being independent and the voxels within one single component are considered as functionally connected to each other. As the stochastic nature of the ICA approach is well-known, we conducted – for the first time on animal data – a pilot investigation to evaluate different numbers of components using the ICASSO algorithm (Himberg et al., 2004). This method is based on running the ICA algorithm many times with slightly different conditions (i.e. bootstrapping and/or varying initial conditions) and taking the results of each run into account to finally give one averaged set of components. This tool allows the visualization of the component clustering and provided a quantitative measure of the robustness of the identified components: the 'quality index' I_q (values ranging from 0 to 1). The index evaluated the compactness and isolation of each cluster, offering the possibility to highlight unstable Independent Component (IC) patterns. The quantitative measures of IC stability obtained with ICASSO facilitated also the final selection of the number of components to be extracted by the algorithm. This is a critical step while using ICA. Based on the former, we present a comparison of 40 and 100-ICASSO results. All mean results are diplayed as spatial color-coded z-maps onto the template. The color coding represents the dependence of the time courses in each voxel compared to the mean time course of the respective component.

Partial correlation (PC) analysis

From the 100-ICASSO results, 8 were excluded as artifactual and a 92 x 92 adjacency partial correlation matrix was calculated to estimate the direct statistical association by controlling correlation mediated by other components (Smith et al., 2010). Negative correlations were further removed (separate analysis needed) and significance of correlation was assessed by using a one sample t-test with thresholding at $p<0.01$, resulting in a weighted undirected matrix (WUM). In order to examine a ranking according number of significant connections, a binary undirected matrix (BUM) was subsequently generated.

Whole brain modular structures

Based on WUM, the community structures of the mouse brain were identified by graph theory and spectral partitioning method including fine tuning (Newman, 2006) to check for stability of the resulting configuration. The clustering coefficient C and the minimum path length L – the two key metrics of small-worldness were computed (Watts and Strogatz, 1998) and compared to the mean clustering coefficient C_{rand} and path length L_{rand} of a random network with the same number of nodes, edges and degree distribution as the rs-fMRI derived network. For a small-world network – as the human brain is shown to be – the ratio C/C_{rand} is defined to be greater than 1 and the ratio L/L_{rand} is approximately 1.

Results and Discussion:

We comparatively present two functional areas associated with cortical (Fig. 1A) and subcortical (Fig. 1B) networks identified with 40-ICASSO and 100-ICASSO. The cortical resting-state cluster, situated at the anatomically well-defined primary somatosensory cortex (SSC), barrel field and secondary somatosensory cortex is representative of the bilateral (bi-hemispherical) pattern of connectivity obtained with 40-ICASSO (Fig. 1 A-a). Refining the analysis with 100-ICASSO (Figs. 1 A-b to e) resulted in separation of the somatosensory cortex functional areas. Unilateral patterns of connectivity were unraveled; indicating that the SSC could have slightly different low frequency fluctuations of the BOLD signal in the two hemispheres. Thus, resting-state networks distinguished in single components from 40-ICASSO were split up in multiple functional circuits when using 100-ICASSO. This was not only relevant for cortical regions but was also a generalized feature of subcortical areas as well. Fig. 1B demonstrates the division of the thalamic networks from one component obtained with 40-ICASSO (Figs. 1 B-f) into 6 functional clusters generated with 100-ICASSO.

Furthermore, 100-ICASSO revealed the functional cortical segregation, splitting this brain area into anatomically meaningful regions (see Figure 2, a) cingulate cortex, b) motor cortex, c) primary somatosensory cortex, d) insular cortex, e) piriform cortex). This refinement with 100-ICASSO could be of high value when conducting studies in animal models of brain disorders for depicting functional abnormalities at specific cortical locations.

Figure 1

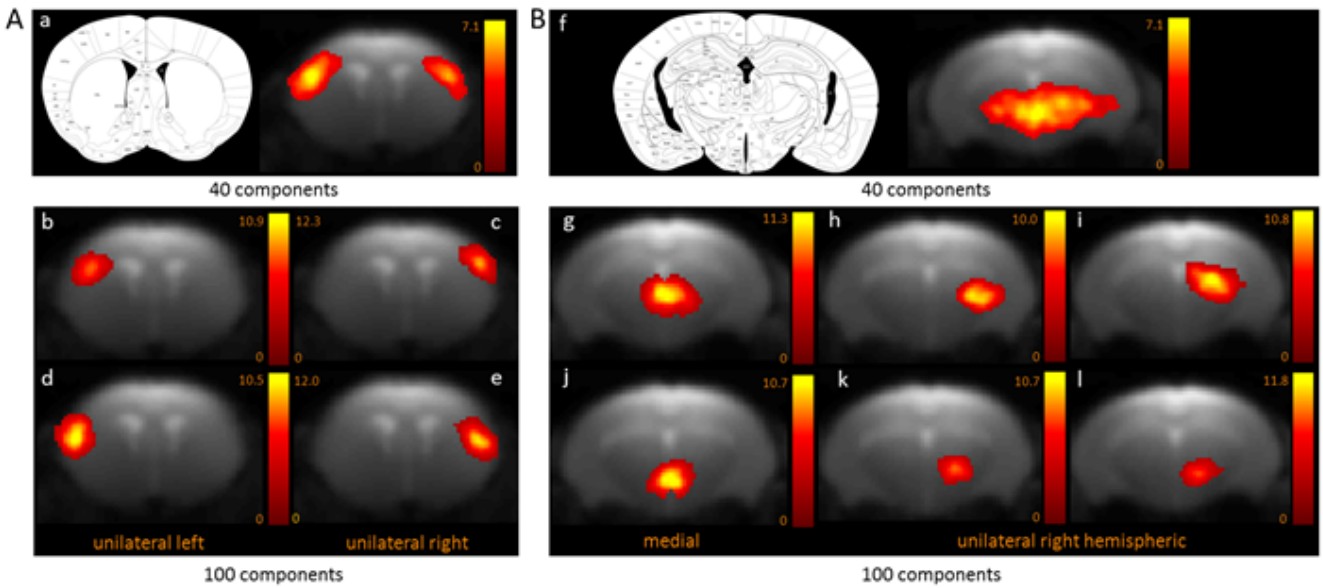

BOLD resting-state fMRI based cortical (A) and thalamic (B) mouse brain functional connectivity clusters, comparatively revealed by 40- (a, f) and 100-ICASSO (b–e and g–l). All images represent spatial color-coded z-maps of the independent components.

Figure 2

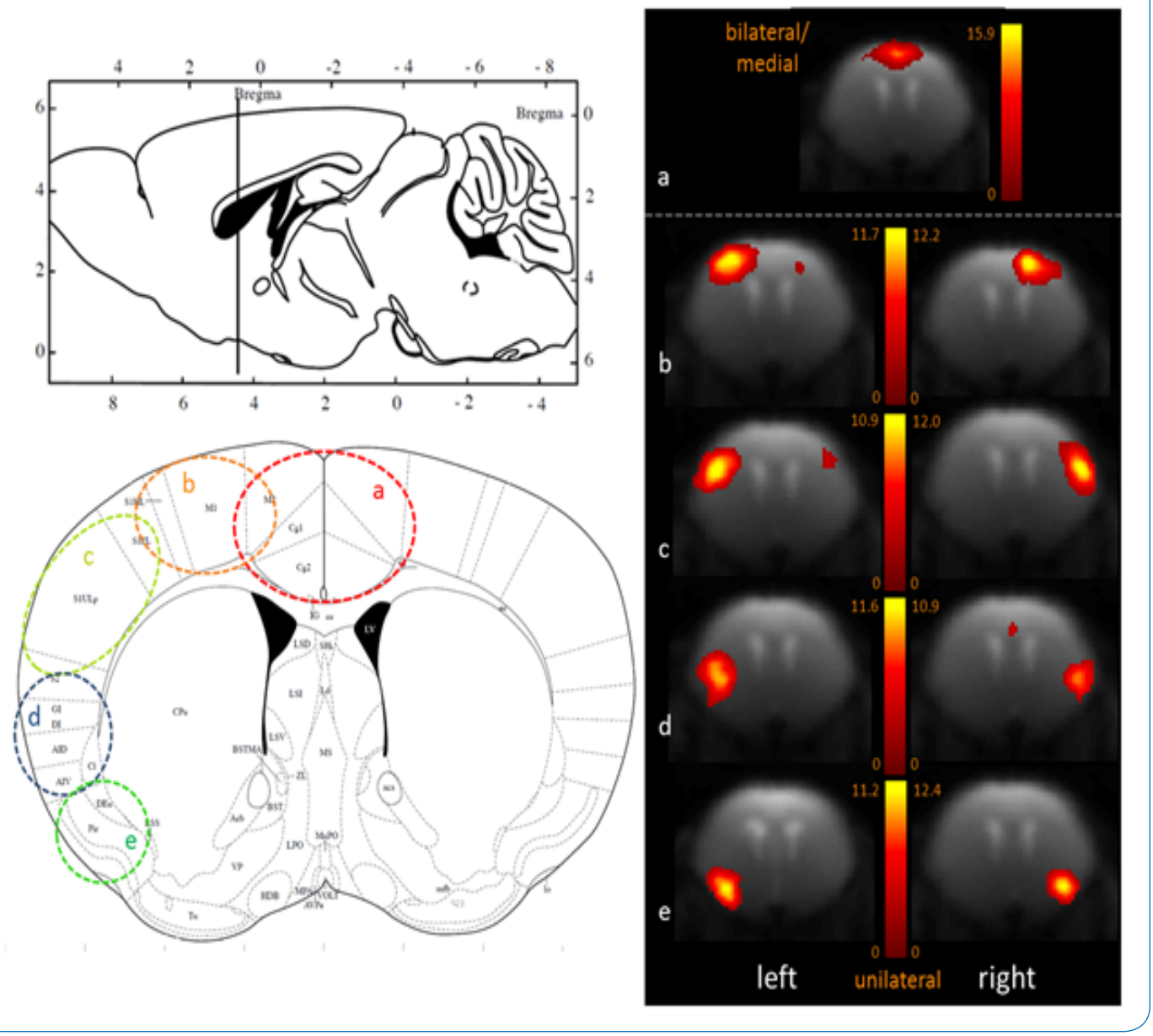

Fine-grained segregation of the cortical mouse brain functional connectivity revealed with 100-ICASSO. Bi- (a) and uni-lateral left and right ICs (b–e), matching well defined anatomical areas (see he atlas axial image - Paxinos and Franklin, 2001) are displayed.

To further evaluate the inter-component connectional relationships and to generate the whole brain connectivity matrix, we calculated the direct connectivity between individual components via PC analysis. The input for our correlation analysis consisted of the 92 non-artifactual resting state clusters (components). The respective 92 x 92 PC coefficient matrix (WUM) averaged across all animals is displayed in Fig. 3A, with respective 3D representation of connectivity in Fig. 3B (positive correlations in red, negative correlations in blue, the components are represented by a dot at their center of mass). The binary undirected matrix (BUM) is displayed in Fig. 3C with 3D representation in Fig. 3D accordingly.

From here, an average number of 11.26 statistically relevant functional connections were calculated for each IC. 47 of 92 resting-state clusters revealed a higher number of relevant connections than average. Because each of these clusters overlap specific anatomical brain area, our method therefore enabled a ranking of the most connected brain regions, considered as nodes of functional connectivity. Fig. 3E provides information regarding the top 13 most connected mouse brain functional areas, ordered according to their respective number of relevant connections. We identified rostro-dorsal Hippocampus as the most connected brain region. One representative MR slice defining the hippocampal network is

presented in Fig. 3F, along with the respective spatial maps of seven of its strongest functional connections. Interestingly, the Hippocampus, as an important part of the limbic system, displayed the highest degree of functional connectivity with brain areas known to be involved in the regulation of behavior, emotion, learning, and memory. Among these regions are retrosplenial cortex, cingulum, amygdala and entorhinal cortex.

The 100-ICASSO functional clusters were also used as nodes, interconnected via edges (inter-components strength from WUM) in the analysis of large scale mouse brain functional connectivity with graph theory. Modularity, global clustering coefficient, mean shortest path length and small-worldness were used to assess topological characteristics of the global network. Based on the data obtained from the WUM, the whole mouse brain network was segregated in five modules to achieve a high modularity value (Q = 0.50). This high Q value suggests a prominent modular structure of intrinsic connectional architecture of the mouse brain. The evaluation of the small-worldness properties of the C57BL/6N mouse brain functional connectivity, a high value of the clustering coefficient, together with a short minimum path length: $C=3.08*C_{rand}$ and $L = 1.11*L_{rand}$. Finally, the ratio value $\sigma = \gamma/\lambda = (C/C_{rand})/(L/L_{rand}) = 3.08/1.11 = 2.77 > 1$, indicates an optimal network configuration for global information transfer and local processing within the mouse brain, corresponding to the small-worldness network configurations.

Comparing our data to the rat study by Liang et al. (2011) we notice higher values of the clustering coefficient $\gamma = C/C_{rand} = 3.08$ in the mouse (vs. 1.7 in the rat, Liang et al., 2011), suggesting a higher level of clustering formation and therefore functional segregation within the mouse. Nevertheless, the ratio of minimum path length ($L/L_{rand} = 1.11$ in mice vs. $L/L_{rand} = 1.08$ in rat) as well as the number of modules (5 in mice vs. 4 in rats with fine-tuning according to the spectral partitioning analysis described by Newman, 2006) are very similar in both species, despite different levels of consciousness during imaging — medetomidine sedated mice vs. awake rats. However, the mouse brain network formed all its modules via complex combination of cortical and subcortical brain areas, whereas Liang et al. could identify modular structures covering exclusively the cortical ribbon of the rat brain.

Figure 3

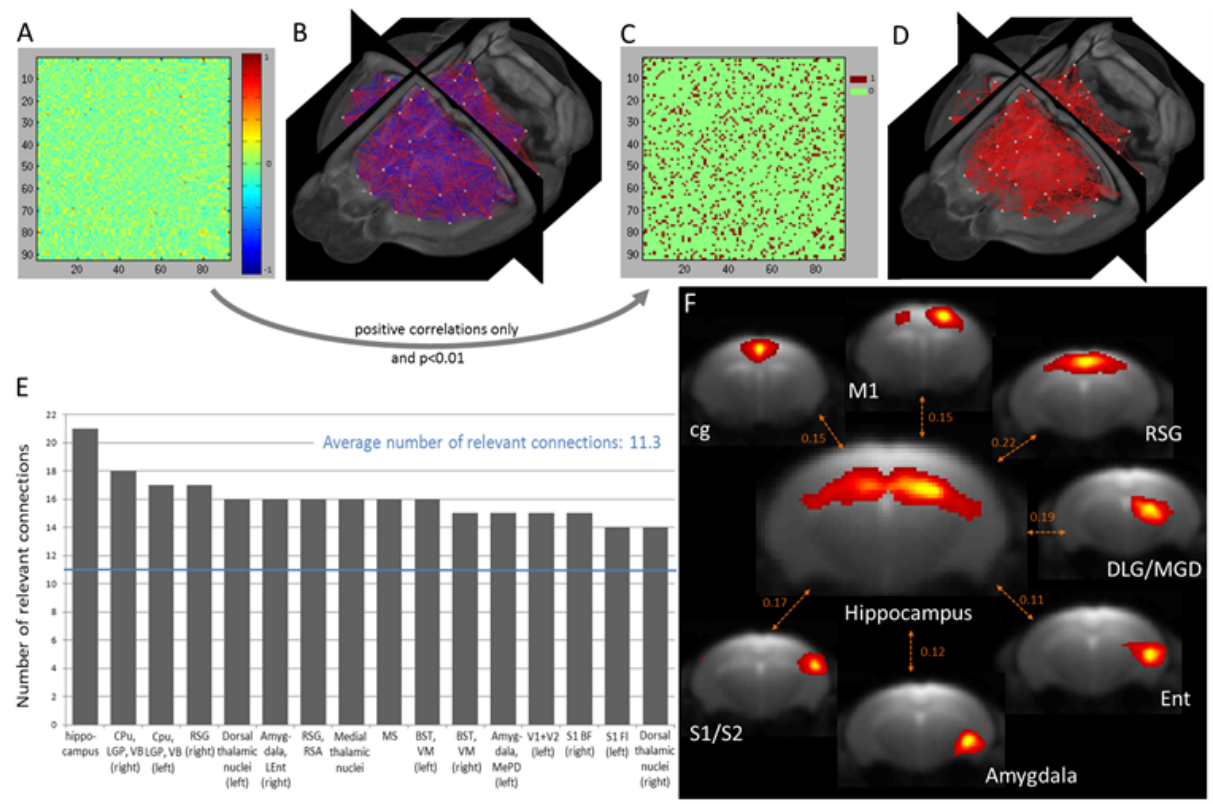

Quantitative assessment of inter-component direct connectivity using partial correlation analysis and identification of the most connected brain regions. (A) Weighted undirected matrix (WUM) generated after correlating the time courses of the non-artifactual components obtained with group 100-ICASSO and respective 3D visualization (B). (C) Binary undirected matrix (BUM) reflecting the statistically significant positive correlations and 3D display (D). (E) Ranking of the most connected brain areas, considered as nodes of the functional connectivity. For identifying the brain regions in the graph see the complete abbreviation list. (F) Spatial maps of the rostro-dorsal hippocampus and of its strongest connections, as reflected by the partial correlation coefficient displayed between pairs of IC.

These results highlight the complex organization of the rodent brain functional connectivity, still conserving the global topological features of a small-worldness network and supporting both segregated/specialized and distributed/ integrated information processing (Bassett and Bullmore, 2006). This seems to be a common feature of healthy rodent and human brains. Therefore, using network topology readouts in animal models of brain pathologies would potentially help in clarifying the mechanisms and the biological substrates of human brain disorders filling the gap between pre-clinical and clinical studies.

Summary and Outlook

Rs-fMRI remains the only methodology able to non-invasively map functional brain connectivity. Here we provide a data acquisition and processing pipeline adapted for studying the mouse brain functional connectivity. This opens an important pathway towards combination of findings at the functional connectivity level with knowledge gained from structural networks investigations via diffusion tensor imaging and fiber tracking (Harsan et al., 2013) as complementary techniques for revealing the full mouse brain "connectome".

References

Bassett DS, Bullmore E (2006), Small-world brain networks. Neuroscientist 12

Biswal B, Yetkin FZ, Haughton VM, Hyde JS (1995), Functional connectivity in the motor cortex of resting human brain using echo-planar MRI, Magn. Reson. Med. 34

Biswal B (2012), Resting state fMRI: a personal history, Neuroimage 62

Calhoun MD, Adali T, Pearlson GD, Pekar J (2001), A method for making group inferences from functional MRI data using independent component analysis, Hum. Brain Mapp. 14

Castellazzi G, Palesi F, Casali S, Vitali P, Sinforiani E, Wheller-Kingshott CA, D'Angelo E (2014), A comprehensive assessment of resting state networks: bidirectional modification of functional integrity in cerebro-cerebellar networks in dementia, Front Neurosci 8

Harsan LA, David C, Reisert M, Schnell S, Hennig J, von Elverfeldt D, Staiger JF (2013), Mapping remodeling of thalamocortical projections in the living reeler mouse brain by diffusion tractography, Proc. Natl. Acad. Sci. U. S. A. 110

Himberg J, Hyvarinen A, Esposito F (2004), Validating the independent components of neuroimaging time series via clustering and visualization, Neuroimage 22

Jonckers E, Van Auderkerke J, De Visscher G, Van der Linden A, Verhoye M (2011), Functional connectivity fMRI of the rodent brain: comparison of functional connectivity networks in rat and mouse. PLoS One 6.

Liang Z, King J, Zhang N (2011), Uncovering intrinsic connectional architecture of functional networks in awake rat brain. J. Neurosci. 31

Mechling AE, Hübner NS, Lee H-L, Hennig J, von Elverfeldt D, Harsan L-A (2014), Fine-grained mapping of mouse brain functional connectivity with resting-state fMRI, Neuroimage 96

Nathan DE, Oakes TR, Yeh PH, French LM, Harper JF, Liu W, Wolfowitz RD, Wang BQ, Graner JL, Riedy G (2015), Exploring variations in functional connectivity of the resting state default mode network in mild traumatic brain injury, Brain Connect 2015

Newman ME (2006), Modularity and community structure in networks, Proc. Natl. Acad. Sci. U. S. A. 103

Odish OF, van den Berg-Huysmans AA, van den Bogaard SJ, Dumas EM, Hart EP, Rombouts SA, van der Grond J, Roos RA (2015), Longitudinal resting state fMRI analysis in healthy controls and premanifest Huntington's disease gene carriers: a three-year follow-up study, Hum Brain Mapp 36

Pawela CP, Biswal BB, Hudetz AG, Schulte ML, Li R, Jones SR, Cho YR, Matloub HS, Hyde JS (2009), A protocol for use of medetomidine anesthesia in rats for extended studies using task-induced BOLD contrast and resting-state functional connectivity, Neuroimage 46

Paxinos G, Franklin K (2001), The mouse brain in stereotaxic coordinates.

Smith SM, Miller KL, Salimi-Khorshidi G, Webster M, Beckmann CF, Nichols TE, Ramsey JD, Woolrich MW (2010), Network modelling methods for FMRI, Neuroimage 54

Sporns O, Tononi G, Kotter R (2005), The human connectome: a structural description of the human brain, PLoS Comput. Biol. 1

Van Essen DC, Smith SM, Barch DM, Behrens TE, Yacoub E, Ugurbil K (2013), The WU-Minn Human Connectome Project: an overview, Neuroimage 80

Watts DJ, Strogatz SH (1998), Collective dynamics of 'small-world' networks, Nature 393

Zhou F, Zhuang Y, Gong H, Wang B, Wang X, Chen Q, Wu L, Wan H (2014), Altered inter-subregion connectivity of the default mode network in relapsing remitting multiple sclerosis: a functional and structural connectivity study, PLoS One 9

www.bruker.com ● **Bruker BioSpin**

info@bruker.com